Aberrant Overexpression of Myosin 1b in Glioblastoma Promotes angiogenesis via VEGF-myc-myosin 1b- Piezo1 Axis

Autor Weifeng Lv
Fourth Military Medical University
Fan Yang
Tianjin Medical University General Hospital, Tianjin Neurological Institute, Ministry of Education and Tianjin City
Zhengmao Ge
Fourth Military Medical University
Lele Xin
Shaanxi Normal University
Lingxue Zhang
Shaanxi Normal University
Qingdong Guo
Fourth Military Medical University
Xinggang Mao
Fourth Military Medical University
Peng Luo
Fourth Military Medical University
Xiaofan Jiang
Fourth Military Medical University
Yanyu Zhang
yanyu.zhang@fmmu.edu.cn
Fourth Military Medical University

Article

Keywords: myosin 1b, GBM, Piezo1, VEGF, myc, tumor vessel

Posted Date: August 4th, 2023

DOI: https://doi.org/10.21203/rs.3.rs-3153199/v1

Additional Declarations: No competing interests reported.

Abstract

Glioblastoma (GBM) is the most aggressive intracranial malignance with poor prognosis, which is attributed to the extreme invasiveness of the tumor. Enhanced angiogenesis is one of the essential hallmarks of GBM, which demonstrates extensive microvascular proliferation and abnormal vasculature. Here, we uncovered the key role of myosin 1b in angiogenesis and vascular abnormality in GBM. Myosin 1b was upregulated in GBM endothelial cells (ECs) compared to their paired non-malignant brain tissue. Knocking down myosin 1b in human/mouse brain endothelial cells inhibited EC migration, proliferation and tube formation. Myosin 1b in ECs are affected by vascular endothelial growth factor (VEGF) signaling through myc. Moreover, myosin 1b promotes angiogenesis via Piezo1 by enhancing Ca^{2+} influx, in which process VEGF can be the trigger. Our results identified myosin 1b as a key mediator in promoting angiogenesis via Piezol1; suggested that VEGF/myc signaling pathway may be responsible for driving the changes of myosin 1b overexpression in GBM ECs.

Highlights

Myosin 1b is overexpressed in endothelial cells of GBM in patients.

Myosin 1b promotes angiogenesis and endothelium integrity.

Myosin 1b regulates angiogenesis via VEGF-myc-myosin 1b-Piezo1 axis.

1. Introduction

GBM is the most common intracranial malignance with devastating prognosis and has not been substantially improved during the last 30 years. Its ability to invade diffusely into brain parenchyma makes it difficult for radical resection. Angiogenesis plays a critical role in GBM progression and aggression, which develops abnormal vasculature and demonstrates extensive microvessel proliferation [1][2]. GBM vessels are usually twisted and highly permeable. GBM cells can migrate along the blood vessels to distant areas or invade their surrounding normal tissues through the highly permeable vessels [3]. The abnormal GBM vasculature express a series of genes in a different way than normal brain vessels [4]. For instance, the expression of tight junction molecules and transporters are decreased in GBM ECs compared to the normal brain tissue [5]. Genes related to vessel permeability that expressed by ECs can be classified into five major subgroups: 1. tight junction molecules, such as *Occludin, Claudin-1, Claudin-3, Claudin-5 Claudin-12, ZO-1* and *ZO-2*; 2. adherens junctions and related molecules (cadherens, PECAM, JAMs, ESAM, connexins, annexins and dystrophin); 3. transcytosis related molecules such as *caveolae* and *clathrim*; 4. transporters such as *FATP-1* and *MFSD2a* which transports fatty acids, *GLUT1* and *SGLT1* which transports glucose, *TfR* a transferrin and *IR* which transports insulin [6]; 5. the extracellular matrix (ECM) enzymes (MMPs). The importance of anti-angiogenic therapy has been recognized during the last decades and has already been applied in clinical practice in several types of cancers [7, 8]. However, anti-angiogenic drug bevacizumab yields modest improvement in GBM treatment

from clinical trials [9]. Therefore, it is fundamental to explore the underlying mechanisms of GBM angiogenesis and looking for new strategies to improve the clinical effects.

Myosin 1b belongs to the myosin superfamily which affects the motility and morphology of cells and once was called myosin-1α or myr1 [10]. Myosin 1b is a single-headed isoform associated with actin which relates to the formation of filopodia, membrane trafficking and the formation of post-Golgi carriers [11]. It is reported that myosin 1b is the most tense-sensitive and widely distributed myosins compared to the other members of the myosin family [12]. Myosin 1b resists mechanical loads and forward motility via binding to actin strongly and keeping stall [13]. The function of myosin 1b has not been understood clearly. Previous studies indicate that aberrant expression of myosin 1b is involved in cancer initiation and progression. Overexpression of myosin 1b derives cancer toward a more migratory phenotype shown in cervical cancer, head and neck squamous cell carcinoma (HNSCC) and prostate cancer [14]. In addition, it was showed that myosin 1b is upregulated in tumors under hypoxia [15] and in the ECs of tumors [16]. Moreover, we found that myosin 1b is upregulated in ECs of GBM [17]. However, the function of myosin 1b in tumor vasculature are poorly understood.

Mechanosensitive ion channel component 1 (Piezo1) was firstly discovered in 2010, which is located on the cell membrane. Piezo1 forms a homotrimer and adoptes a triple-blade propeller-like structure [18]. Piezo1 is widely expressed in cells of various tissues, which is the ion-conduction pore-formation subunit of mechanically activated (MA) ion channels [19]. The function of Piezo1 is to sense environmental signals especially mechanical forces and then activates and ensues intracellular downstream signal pathways such as: 1. induction of adenosine triphosphate (ATP) release, which subsequently activates purinergic P2X and P2Y receptors and removes ATP by ATP-scavenging ectonucleotidases; 2. activation of calpains, which induces Ca^{2+} influx to arouse a series of cellular responses [20]. Piezo1 has been confirmed to participate in cell proliferation, migration and angiogenesis [21][22]. Myosin1 superfamily are actin-based motors which participate in membrane tense sensing and transduction [23]. It has been reported that myosin1c forms clusters to maintain enough tension for opening of Ca^{2+}-dependent transduction channels [24]. Myosin1b, as a contractive and tense-sensitive superfamily member of myosins, was found to promote EC migration and tube formation by our study, which activates us to explore the relations between myosin1b and Piezo1 [25][26].

In the present study, we explored the mechanisms behind the aberrant overexpression of myosin 1b in ECs of GBM compared to the normal brain, examined the function of myosin 1b in angiogenesis and vascular integrity. We clarified that VEGF/myc could be the underlying signaling pathways which lead to aberrant overexpression of myosin 1b in GBM ECs. Furthermore, we demonstrated that myosin1b promotes angiogenesis by enhancing Piezo1 expression as well as Piezo1-mediated Ca^{2+} influx. Thus, we suggest that myosin1b plays a pivotal role in GBM angiogenesis and vascular abnormality through VEGF-myc-myosin 1b-Piezo1 axis. Our study is the first step to explore the relationship between myosin 1b and GBM vasculature, which may shed lights on new anti-angiogenic strategies for GBM patients.

2 .Methods

2.1 Cell lines and culture

The immortalized murine bEnd.3 brain endothelial cell line and human umbilical vein endothelial cell (HUVEC) line was provided by Shaaxi Normal University (Xi'an, China). Cells were cultured in Endothelial Cell Medium (ECM) (1001, ScienCell, California, MA, USA), or Dulbecco's Modified Eagle's Medium (DMEM) with 4500 mg/L d-glucose, 110 mg/L sodium pyruvate, 1.5 g/L sodium bicarbonate, and L-glutamine (31053028, Thermo Fisher Scientific, Waltham, MA, USA), supplemented with 10% fetal bovine serum (10099141C, Thermo Fisher Scientific, Waltham, MA, USA), 100 units/mL of penicillin, and 100 µg/mL of streptomycin (15140122, Thermo Fisher Scientific, Waltham, MA, USA). Cells are maintained in a humidified incubator at 37°C with 5% CO_2 and 95% air. All experiments were carried out when the density of cells were 80–90% of confluence.

2.2 Bioinformatics Analysis of myosin 1b Expression in ECs

Single cell RNA sequencing (scRNA-seq) datasets of ECs from GBM and paired non-malignant control brain tissue were downloaded from the Gene Expression Omnibus (GEO) database (GSE162631). Information for cells and samples were obtained in the previous study [17]. Four hundred and sixteen ECs from peripheral endothelial cell type I (Pe1) cluster were considered as nonmalignant brain endothelial cells. Six hundred and thirty-four ECs from tumor core endothelial cell type I (Co1) and tumor core endothelial cell type II (Co2) clusters were considered as tumor endothelial cells.

2.3 Animals, patients tissue and experimental applications.

C57BL6 Gtva;Arf-/- mice were generated by Eric Holland and provided by Lene Uhrbom (Uppsala University). All experimental applications were carried out in accordance with ARRIVE guidelines. Mice were housed in specific pathogen free (SPF) barrier facilities. C57BL6 Gtva;Arf-/- female mice were randomly separated into two groups as control group and orthotopically transplanted group. RCAS-producing DF-1 cells (RCAS-PDGFB-HA) were orthotopically transplanted by stereotaxic injection of 105 cells into 6–8 weeks old mice to induce GBM as described in the previous publication [27]. The control group were injected with equivalent phosphate-buffered saline (PBS). Mice in all groups were decapitated under anesthesia via intraperitoneal administration of ketamine (75 mg/kg) plus xylazine (10 mg/kg). Mice were sacrificed upon symptoms of illness or at the endpoint of 15 weeks post-injection and were perfused intracardially with 4% cold paraformaldehyde phosphate buffer (PFA, pH 7.4). Mice brain were incubated with 4% PFA (pH 7.4) for 4 hours at room temperature, dehydrated by 20%-30% sucrose for 24 hours at 4°C, and then were frozen in OCT Cryomount (4583, Sakura Tissue-Tek, Torrance, CA, USA) for ulteriorly immunohistochemical staining of myosin1b and CD31. All animal experiments were conducted in compliance with relevant laws and institutional guidelines, and approved by the Laboratory Animal Welfare and Ethics Committee of Fourth Military Medical University (permit 20220897).

For Human, patient samples were collected from GBM patients after tumor resection surgery immediately at Xijing Hospital which contains the tumor tissue and adjacent normal tissue. The research protocol was performed following the principles of the Declaration of Helsinki. All patients provided their informed

consents, and the whole process was monitored by the medical ethics office of Xijing Hospital. Patient samples were incubated with 4% PFA (pH 7.4) for 24 hours at room temperature, dehydrated by 20%-30% sucrose for 24 hours at 4°C, and then were frozen in OCT Cryomount (4583, Sakura Tissue-Tek) for ulteriorly immunohistochemical staining of myosin1b and CD31. Ethical permission for using patient samples was granted by the Medical Ethics Committee of Xijing Hospital (KY20193098).

2.4 Reagents and plasmids

Dimethyl sulfoxide (DMSO) was purchased from Xi'an Kehao Bioengineering (DH105-2) (Xi'an, China). Lentivirus plasmids targeting mice or humans containing full-length myc (EX-myc-pEZ-Lv105), myosin 1b (EX- Myosin 1b-pEZ-Lv151) or their corresponding empty cherry plasmids (EX-pEZ-Lv105 and EX-pEZ-Lv151) were purchased from Guang-zhou Fulengen (Guangdong, China). Short hairpin myc targeting mice or humans and its empty scrambled plasmid (CSHCTR001-LVRU6P), as well as short hairpin myosin 1b targeting mice or humans and its empty scrambled plasmid (CSHCTR001- LVRU6GH) were purchased from Guangzhou FulenGen.

2.5 Transient transfection

The cells were seeded into six-well plates and transfected with individual plasmids or siRNAs using lipofectamine 2000 (11668019, Thermo Fisher Scientific) followed by the manufacturer's instructions.

2.6 Cell proliferation assay

bEnd.3 and HUVEC cells were seeded at the density of 1,000 cells/well in 96-well plates in septuplets. Cell proliferation was estimated using the CCK8 kit (k1018, Apexbio, Boston, MA, USA). To each well, 10 μL CCK-8 solution were added, the cells were then incubated for 3 hours at 37°C. The absorbance at 490 nm was measured by using a microplate reader (SH-9000; Hitachi, Tokyo, Japan).

2.7 Western blot analysis

Cells were lysed in radioimmunoprecipitation assay (RIPA) buffer (50 nM Tris-HCl, 150 nM NaCl, 1% NP40, 0.1% sodium dodecyl sulfate (SDS), 0.5% deoxycholate, and 1 mM phenylmethanesulfonylfluoride) for 30 minutes on ice. A total of 30 μg protein was separated by gradient SDS-polyacrylamide gel electrophoresis (SDS-PAGE) (4%-12% polyacrylamide). Proteins were then transferred to nitrocellulose membranes. The membranes were blocked, immunoblotted with the indicated primary antibodies, and subsequently incubated with the corresponding horseradish peroxidase (HRP)-conjugated secondary antibodies. The signals were detected with the enhanced chemiluminescence system (Tanon 5500, Tanon Science and Technology, Shanghai, China). The following commercial antibodies were used: rabbit anti-VE-cadheren (ab205336, Abcam, Cambridge, UK), rabbit anti-E-cadheren (3195T, Cell Signaling Technology, Danvers, MA, USA), rabbit anti-MMP1 (ab134184, Abcam), rabbit anti-MMP9 (ab76003, Abcam), rabbit anti-MMP14 (ab51074, Abcam), rabbit anti-ANXA1 (32934T, Cell Signaling Technology), rabbit anti-ANXA5 (8555S, Cell Signaling Technology), rabbit anti-ANXA6 (29015S, Cell Signaling Technology), rabbit anti-ANXA10 (ab213656, Abcam), rabbit anti-connexin 4 3 (83469T, Cell Signaling Technology). rabbit anti-GAPDH (5174S, Cell Signaling Technology), rabbit anti-myosin 1b (EPR16223,

Abcam), rabbit anti-myc (9402S, Cell Signaling Technology), and HRP-anti-rabbit IgG (7074, Cell Signaling Technology).

2.8 Quantitative real-time PCR analysis

Total RNA was extracted from bEnd.3 and HUVEC cells by using RNAiso Plus (9109 Takara Bio,Kusatsu, Japan). The One-Step SYBR PrimeScript RT-PCR Kit (RR820A Takara Bio) was used for qRT-PCR detection of myosin 1b, myc, or β-actin. The qRT-PCR was conducted by using a Bio-Rad C1000 thermal cycler with the following conditions: 95°C for 3 minutes, followed by 40 cycles of 95°C for 15 seconds and 60°C for 30 seconds. The primers used in this study were synthesized by Beijing Genomics Institute, and their sequences are listed in the supplement table1 and table 2. The expression levels were calculated relative to β-actin as the endogenous control. Relative expression was calculated as $2^{-(\text{Ct test gene} - \text{Ct ACTB})}$

2.9 Immunohistochemical staining of mouse and patient samples

Five micrometer tissue sections of mouse or human patient samples were cut with a Leica cryostat sectioning machine. Tissue sections were incubated overnight at 4˚C with primary antibodies, followed by incubation with Alexa Fluor-labeled secondary antibodies for 1 h at room temperature and mounted by DAPI Staining Solution (ab228549, Abcam). Images were acquired through 40× or 20× objectives by Zeiss Axio Imager M2 microscope. The following antibodies were applied: anti-mouse CD31 (1:500, MA3105, Thermo Fisher Scientific), anti-human CD31 (1:500, AF806, R&D Systems, Minnesota, USA), rabbit anti-myosin 1b (1:200, ab194356, Abcam), goat anti-armenian hamster Alexa 568 (ab175716, Abcam), donkey anti-sheep Alexa 555 (A-21436, Thermo Fisher Scientific), and donkey anti-rabbit Alexa 488 (ab150073, Abcam).

2.10 Wound healing assay

For the wound healing (scratch wound) assay, 2×10^5 cells/well (three wells per group) were plated into a 6-well plate and incubated to reach the confluence. The monolayer was scratched by using a fine pipette tip and washed with serum-free medium to remove detached cells. The cells were then cultured in complete ECM medium supplemented with half of the serum supply concentration. Cells were photographed at 12 h post-wounding. The closure area of wound was calculated as follows: migration area (%) = $(A^0 - A^n)/A^0 \times 100$, where A^0 represents the area of initial wound area, A^n represents the remaining area of wound at the metering point.

2.11 Transwell permeability assay

Transwell insert (0.8μm, for 24-well plate) (3422, BD bioscience, Franklin Lakes, NJ, USA) were coated with ECM gel (3536-005-02, R&D) and incubated for 3 hours in incubator. Approximately 3000 cells of bEnd.3 or HUVEC were seeded in the transwell. Sixteen hours post seeding, the cells were transiently transfected with lentivirus plasmids containing full-length of myosin 1b or their corresponding empty cherry plasmids, and 36 hours post transfection, the medium of the upper chamber is changed to be

medium containing 0.5% fluorescent- microsphere (234340, Sigma Aldrich). Two hours later, take 100 μL medium per well to measure. The permeability was calculated as follows: permeability rate (%) = $A^n/A^0 \times 100$, where A^0 represents the fluorescence absorbance value of the medium from the upper chamber, A^n represents the fluorescence absorbance value of the medium in the wells.

2.12 Transwell migration assay

Transwell migration assay was performed by using transwell inserts (3422, BD bioscience) with a filter of 8 μm pore which were coated with ECM gel (3536-005-02, R&D). 4×10^4 cells in serum-free medium were seeded into the upper chamber of the insert and complete medium was added to the lower chamber. After 36 h incubation, the cells were fixed with methanol and stained with Giemsa. Then cells on the top surface of the membrane were wiped off, and cells on the lower surface were examined with Zeiss Axio Imager M2 microscope at 20× magnification. 4 random fields were photographed for counting purposes and the average number of migrated cells was used as a measure of migration capacity.

2.13 Immunofluorescent staining of endothelial cells

Endothelial cells cultured on coverslips were fixed, permeabilized and followed by blocking as previously described. The cells were then stained with Phalloidin-iFluor 488 (ab176753, Abcam) for 1 hour at room temperature, and nucleus was stained with Hoechst 33258 (94403, Sigma-Aldrich).

2.14 Intracellular calcium content detection

Endothelial cells were cultured at 6-well plates. Change medium at the confluence of 80% and incubate the cells in a humidified incubator at 37°C with 5% CO_2 and 95% air. After 24 hours incubation, wash the cells with PBS and then the intracellular calcium was determined according to the manufacturer's procedure of the intracellular calcium content detection kit (s1603s, Beyotime).

2.15 Tube formation assay

In vitro tube formation assay was performed by using the Angiogenesis Assay Kit (Abcam, AB204726) according to the manufacturer's procedure..

2.16 Image Analysis

Imaging of immunofluorescent staining was done by using the Zeiss Axio Imager M2 microscope and the ZEN 3.5 software. Images were analyzed by using the Image J 1.45s software (National Institute of Health, Bethesda, MD, USA).

2.17 Statistical analysis

Statistical analysis was performed by using GraphPad Prism software and R software. For comparison of two-group dataset, 2-sided, unpaired t-test was applied. In this study, n represents individual samples. Error bars in the graphs represent the standard deviation (SD). Statistical significance was defined as $P < 0.05$, *; $P < 0.01$, **; $P < 0.001$, ***; $P < 0.0001$, ****.

3. Results

3.1 Myosin 1b is upregulated in the endothelial cells of GBM

To investigate the expression of myosin 1b in GBM ECs, we reanalyzed a recently published dataset of scRNA-seq of ECs from tumors and its paired nonmalignant brain tissue in 4 GBM patients (Student's t-test; $p < 0.0001$) [17] (Fig. 1A). Upregulation of myosin 1b in tumor vasculature was further confirmed at protein level by immunohistochemical staining of patient GBM and mouse GBM samples (Fig. 1B-1C). Taken together, these results demonstrated that myosin 1b is upregulated in GBM ECs, which indicates that myosin 1b may play a crucial role in GBM vasculature.

3.2 Myosin 1b promotes angiogenesis and protects the integrity of endothelium

To investigate whether myosin 1b affects angiogenesis, we chose two endothelial cell lines for further study. Mouse brain endothelial cells (bEnd.3) and human endothelial cells (HUVEC) cells were transfected with siRNA to knock down myosin 1b. Then the ability of cell migration and proliferation were examined. The knockdown efficiency of myosin 1b was confirmed by real time PCR and western blot (Fig. 2A and 2B). The ECs transfected with myosin 1b siRNA exhibited poorer ability in migrating examined by wound healing assay and transwell migration assay (Fig. 2C and 2D). CCK-8 assay revealed that the proliferating ability of the ECs with myosin 1b knocking down is decreased compared to the control (Fig. 2E). In addition, tube formation assay was performed, which showed that myosin1b promotes angiogenesis (Fig. 2F). Therefore, our findings suggest that myosin 1b promotes angiogenesis.

To mimic the situation of myosin 1b overexpression in the GBM ECs which has been shown in patients and to identify the function of myosin 1b in GBM vasculature, bEnd.3 (mouse brain) and HUVEC (human) ECs were transfected with plasmids for myosin 1b overexpression (ORF). Transwell permeability assay was then performed. The permeability readout (ratio of fluorescence) was normalized to the negative control group which was coated with only ECM but no cells. The results showed less transmigrated fluorescent-microsphere in the myosin 1b overexpressed endothelial cells, which indicate that myosin 1b promotes vascular integrity (Supplemental Fig. 1A). Overexpression of myosin 1b in bEnd.3 and HUVEC cells were confirmed by real-time PCR in comparation with their corresponding empty plasmids transfect group (Supplemental Fig. 1B). To further explore the mechanisms that myosin 1b overexpressing promotes vascular integrity, we selected and checked 36 genes which are related to the vesssel integrity. These molecules in maintaining the integrity of blood vessels can be classified to five major subgroups: the tight junction molecules (*occludin, claudins*, and *ZO*), transcytosis (*caveolae* and *clathrim*), transporters (*MFSD2a, FATP1, GLUT1, SGLT1* and *TfR*), the adherens other junctions (*cadherens, PECAM, JAMs, ESAM, connexins, annexins* and *dystrophin*), and the ECM enzymes (*MMPs*) which can degrade basement membranes of the vessel [28]. According to our results, the transcriptional level of *claudin1, claudin12, Zo2, Mmp1, Mmp9, Mmp14, Fatp1, Sglt1, Glut1, TfR, VE-cadheren, E-cadheren, Dystrophin,*

Connexin hemichannels Cx30, Jam-A, Cx43, Annexin5 and *Annexin12* were enhanced in mouse brain ECs; and the level of *occludin, claudin3, claudin12, ZO1, MMP1, MMP9, MMP14, FATP1, SGLT1, TfR, VE-cadheren, Dystrophin, Connexin hemichannels CX30, JAM-A, JAM-B, PECAM-1, CX43, ESAM, Annexin5* and *Annexin12* were enhanced in human ECs, both of which indicates that myosin 1b is involved in vascular integrity in an overall protecting manner (Supplemental Fig. 1C-1F).

We also checked some of the gene changes upon myosin 1b overexpression at the protein level. They are E-cadheren, VE-cadheren, MMP1, MMP9, MMP14, Annexin 1, Annexin 3, Annexin 5, Annexin 6, Annexin 10 and connexin 43. Western blot assay verified that myosin 1b promotes the expression of E-cadheren, VE-cadheren, MMPs, Annexins and connexin 43 in both human and mouse ECs, while MMP1, Annexin 5 and 10 are upregulated in only human ECs; MMP1, MMP9, Annexin 3, 5, 6, and 10 are upregulated in only mouse brain ECs. These results indicate that myosin 1b participates actively in protecting the integrity of endothelium.

Above all, our findings indicate that myosin 1b promotes angiogenesis and shows an overall protection function in vascular integrity.

3.3 VEGF promotes myosin 1b expression in ECs, of which pathway myc is indispensable

We next explored which signaling pathway might be involved in mediating myosin 1b overexpression in GBM ECs. Hypoxia takes place frequently in tumors including GBM due to the conflicts between rapid tumor growth and insufficient blood vessels and triggers gene expression changes. Vascular endothelial growth factor (VEGF) is a key responding molecule to hypoxia [29], which plays critical roles in vasculogenesis during embryonic stages and angiogenesis in the adults [30]. We have shown that myosin 1b is upregulated in the ECs of GBM compared to the normal brain. We therefore speculated and investigated if VEGF signaling mediates myosin 1b expression in GBM ECs. We analyzed the expression of myosin 1b in both bEnd.3 and HUVEC cells upon stimulation of VEGFA. Cells were treated with VEGFA at different concentration for different time length. The effects of VEGFA on myosin 1b reaches the maximum at the concentration of 25 μM for 48 hours in HUVEC and the same concentration for 24 hours in bEnd.3 cells (Fig. 3A), of which conditions were used in the following experiments. Both western blot analysis showed that VEGFA promotes myosin 1b expression in human and mouse brain ECs (Fig. 3B).

The downstream signaling of VEGF which regulates myosin 1b expression in brain ECs is still unknown. By analyzing the structure of *MYOSIN* promoter, it is suggested that *MYOSIN* contains binding sites for Myc, Max, CEBPB and GATA-2 at the promoter region according to the previous study [31]. Among all the binding motifs, Myc caught our sight. Myc, a crucial transcription regulator, involves in various physiological process including genetic control of aging, apoptosis, stress resistance and energy efficiency. Importantly, it is also an oncogene that has been implicated in GBM tumors [32]. We therefore investigated if myc is functioning as a transcription factor to modulate myosin 1b expression. We performed transient transfection to bEnd.3 and HUVEC cells to establish myc overexpression or knockdown in ECs. The results show that the protein expression of myosin 1b was increased by

overexpressing myc and decreased by knocking down myc in both human (Supplemental Fig. 2A and 2B) and mouse brain (Supplemental Fig. 2C and 2D) ECs. We also confirmed this at the transcriptional level by qualitative real-time PCR (Supplemental Fig. 2E for human ECs and 2F for mouse ECs). These results suggested that myc is a transcription factor for myosin 1b expression in brain ECs. Interestingly, we could show that myc is responding simultaneously as myosin 1b by VEGFA stimulation (Fig. 4A-4B). To determine whether VEGF stimulated myosin 1b upregulation in ECs is via myc, myc was knocked down in HUVEC and bEnd.3 cells respectively and the cells were then treated with VEGFA. We could show that the effect of VEGFA on myosin 1b is diminished when myc is lacking (Fig. 4C). The results from the real-time PCR are consistent with western blot assay (Fig. 4D). Therefore, we conclude that VEGF promotes myosin 1b expression in ECs via myc. Our results suggest that activated VEGF signaling could be the reason for myosin 1b overexpression in GBM ECs, in which process myc is involved.

3.4 Myosin 1b promotes both Piezo1 expression and the calcium influx in ECs and VEGFA can be the trigger

Myosin 1b is a slow tense-sensing motor depolymerase, belongs to the myosin superfamily of actin-based motors which were found to take part in membrane tense sensing and transduction [23]. Piezo1 is located on the cell membrane and transmits mechanical stimuli into biological cues, which induces calcium influx to promote cell proliferation and migration [19]. In addition, Piezo1 has been reported to promote angiogenesis [33]. Therefore, we explored if myosin 1b promotes angiogenesis via Piezo1.We first established cell lines with stable myosin1b overexpression or knockdown. We examined the expression of Piezo1 by WB assay and found that Piezo1 was upregulated by myosin 1b overexpression and suppressed when myosin1b was knocked down (Fig. 5A-5B). The RT-PCR results were consistent with the WB assay, both of which suggested that Piezo1 is regulated by myosin 1b (Fig. 5C-5D). Piezo1 is known as a mechanosensitive ion channel. We have shown that myosin 1b affects Piezo1 expression. Therefore, we would like to check if the ion influx especially the Ca^{2+} in the ECs are affected by myosin 1b stimulated changes of Piezo1. To explore this, intracellular level of calcium were detected in cells with constitutive myosin 1b overexpression or knockdown, by which we could show that the Ca^{2+} influx were associated with myosin 1b induced Piezo1 expression. To investigate if VEGFA has a similar effect on the Ca^{2+} influx in the ECs since we have shown that VEGFA upregulates myosin 1b, cells were treated with VEGFA for 48 hours (for HUVEC) and 24 hours (for bEnd.3), we could see that VEGFA upregulates Ca^{2+} influx in the ECs and knockdown of myosin 1b diminished the effect (Fig. 5E). These results identified that myosin 1b promotes Piezo1 expression and Ca^{2+} influx in ECs, and VEGFA can be the trigger.

3.5 Myosin1b promotes angiogenesis via Piezo1 and VEGFA could be the trigger

We further explored the mechanisms of the effect that myosin1b promotes angiogenesis. HUVEC and bEnd.3 cells were treated with Piezo1 channel agonist (yoda1) or antagonists (dooku) at different concentrations for 48 hours (HUVEC) or 24 hours (bEnd.3), which is the optimal time of VEGFA treatment identified preciously. Then the level of calcium content is examined. It’s found that the effect of Yoda1

reaches the maximum at the concentration of 2μM for HUVEC and 4μM for bEnd.3 and the effects of dooku1 reaches the maximum at the concentration of 4μM for HUVEC and 2μM for bEnd.3, which concentrations were used for further examination (Fig. 6A-6B). To identify if myosin 1b mediated EC tube formation is dependent on Piezo1 activity, HUVEC or bEnd.3 cells with constitutive myosin1b overexpression or knockdown were treated with yoda1 or Dooku1 when the tube formation assay was performed. The results showed that EC tube formation was inhibited by lacking of myosin 1b but was rescued when yoda1 was added. In consistent with this, overexpression of myosin 1b promoted EC tube formation, but the effect was abolished when adding dooku1 (Fig. 6C-6D). These results demonstrated that myosin 1b induces EC tube formation via Piezo1. We have also checked if VEGFA induces EC tube formation through myosin 1b, since we have shown that myosin 1b was regulated by VEGFA. To identify this, ECs with or without constitutive myosin1b knockdown were treated with VEGFA when tube formation assay was performed. According to the results, we could show that VEGFA induces EC tube formation which is dependent on myosin 1b. Thus, we could reach the conclusion that VEGFA promotes EC tube formation via myosin 1b, which exerts its effect through activating Piezo1. Above all, we suggest that myosin 1b promotes angiogenesis via activating Piezo1, in which process VEGFA could be the trigger.

4. Discussion

Increased angiogenesis is a hallmark of GBM [34]. GBM vessels are abnormal which is usually tangled, unorganized, highly permeable and leaky, significantly larger in diameter, and with thickened basement membrane [35]. Vessels provide oxygen and nutrients for tumor growth and also guide tumor cell migration [36]. The extent of glioma vascularization is consistent with the malignant degree of tumors and the prognosis [37]. Therefore, anti-angiogenic therapy is considered as an important strategy for GBM although it was failed in the phase- clinical trials [38]. Side effects such as limited approach of anti-angiogenic drugs appeared after a temporary remission of the cancer by using bevacizumab [9]. To focus on neovessel normalization, blood flow restoring and vessel permeability inhibition of anti-angiogenic therapy, and to combine with other therapeutics, may provide benefits, for example to promote immune cells to infiltrate and take functions or benefit drug delivery [39]. Deep insights and novel therapeutic strategies to improve anti-angiogenic treatment is in urgent needs.

In this study, we focused on myosin 1b, an aberrantly expressed protein in the ECs of GBM compared to the normal brain, to explore its function on GBM vessels. Myosin 1b belongs to the myosin superfamily that affects the motility and morphology of cells [10][13], which is located at the membrane ruffles to connect the actin cytoskeleton with the membrane [40][41]. Myosin 1b is associated with the actin filament translocation, in which process the motility function of myosin 1b is regulated by calcium ion by binding to the IQ motifs of myosin 1b [13][27][42][43]. The slow kinetics ensures myosin 1b to modulate actin rearrangement by responding to tense stimulation [44][45]. Moreover, myosin 1b is widely involved in the proliferation, migration, and filipodia formation of cells [13]. Previous studies indicated that myosin 1b regulates the initiation and progression of various tumors such as cervical cancer, head and neck squamous cell carcinoma and prostate cancer [14][46]. In addition, negative association between myosin 1b expression and the prognosis of GBM patients has been reported [47]. In contrast, our study has been

focused on the ECs other than tumor cells. We could show that myosin 1b is upregulated in GBM ECs. To explore the relationship between myosin1b and angiogenesis, experiments were carried out to demonstrate that myosin1b can promote EC proliferation, migration, and tube formation. In addition, we have elucidated the function of myosin 1b in protecting vessel integrity. We showed that there are less fluorescent microspheres passing through the EC layers when myosin 1b is overexpressed. We also checked the vascular permeability related genes affected by myosin 1b, which showed that myosin 1b regulates the gene expression of *VE-cadheren, E-cadheren*, *GLUT1, MFSD2a, MMPs*, etc. Both results suggest myosin 1b promote endothelium integrity. Above all, our findings provide new understanding of the role of myosin 1b in GBM angiogenesis and vascular integrity. Hypoxia is considered as the key factor to trigger angiogenesis [48]. VEGF is an important mediator of hypoxia-induced angiogenesis [49]. A previous study indicated that myosin 1b expression is upregulated under hypoxia [15]. We have shown that myosin 1b is upregulated in the ECs of GBM which could be often under hypoxic situation. Therefore, VEGF signaling has drawn our attention to connect to the aberrantly expressed myosin 1b in GBM ECs. We could show that VEGF stimulates myosin 1b expression. To further uncover the downstream mediator of VEGF which regulates myosin 1b, we proposed myc as the transcription factor based on the structure of myosin 1b promoters by one study [31]. In addition, myc is a widely accepted transcription regulator in a plenty of tumors including GBM [50], which regulates gene expression via binding to the promoters involved in the process of proliferation, migration and invasion [51]. Moreover, myc has been implicated in VEGF signaling in a previous study [52]. Therefore, we have checked if myc is involved in VEGF induced myosin 1b expression. Firstly, we demonstrated that myc is essential for myosin 1b expression in ECs. And then we showed that the upregulation of myosin 1b by VEGF stimulation can be blocked by knocking down myc. These together revealed that myosin 1b in ECs is modulated via VEGF-myc-myosin 1b axis.

The underlying mechanism behind myosin1b induced angiogenesis remains to be identified. We focused our sight on a mechanosensitive ion channel component named as Piezo1. Piezo1 belongs to the piezo superfamily. The function of piezo family was firstly found in 2010 [53], which is to translate mechanical stimuli into biological cues and then induce the calcium influx. In most mammals, Piezo1 is widely expressed in a variety of organs and tissues which faces extra mechanical stimuli such as lung, skin and kidneys [53]. Piezo1 plays critical roles in angiogenesis. According to the publication, global Piezo1 knockout mice exhibit lethal pathological vessel formation, dying at 14.5 weeks after production for poor circulation [21]. In adults, Piezo1 assembles in ECs to sense the blood pressure and control the release of nitric oxide (NO) to maintain proper perfusion [21]. It is recognized that Piezo1 is an indispensable loop in angiogenesis. However, the mechanism is still in need of further investigation. We suggested Piezo1 as the downstream molecule in myosin1b induced angiogenesis based on the following facts: myosin1b is a contractive tense-sensing motor [23]; Piezo1 as a mechanosensitive ion channel was involved in angiogenesis[21]. In our study, we for the first time identified that myosin1b can upregulate Piezo1 at both transcriptional and protein level. In addition, the Ca^{2+} influx in ECs is positively regulated by myosin1b expression level, which indicates that myosin1b may affect the ion channel activity of Piezo1. VEGFA can also promote Ca^{2+} influx in ECs which is mediated by myosin 1b. In order to identify whether myosin1b promotes angiogenesis through Piezo1, tube formation assay was performed on ECs with or

without constitutive myosin1b knockdown or overexpression when treated with VEGFA, Yoda1 (piezo1 agonist) or Dooku1 (piezo1 antagonist). According to the results, we concluded that myosin1b promotes angiogenesis through modulating Piezo1 activity, and VEGFA could be one of the upstream stimulators of this process.

Taken together, our data suggested the key role of myosin 1b in GBM angiogenesis and vascular integrity and identified the underlying mechanisms.

Abbreviations

GBM, glioblastoma; FBS, fetal bovine serum; IHC, immunohistochemistry; mAb, monoclonal antibody; NC, negative control; PCR, polymerase chain reaction; SD, standard deviations; shRNA, short-hairpin RNA; ECs, endothelial cells; VEGF, vascular endothelial growth factor; ECM, extracellular matrix; scRNA-seq, single cell RNA sequencing.

Declarations

Data availability:

All data generated or analysed during this study are included in this published article [and its supplementary information files].

Author Contributions: Conceptualization, W.L. and Y. Z.; Methodology, W. L., F.Y., X.J., and Y.Z.; Software and validation, W. L., F.Y., Z.G., X.L., L.Z., Q.G. X.M., P.L., X.J., and Y.Z.; Formal analysis, W. L., F.Y., Z.G., X.L., L.Z., Q.G. X.M., P.L., X.J., and Y.Z.; Investigation, W. L., F.Y., Z.G., X.L., L.Z., Q.G. X.M., P.L., X.J., and Y.Z.; Resources, W. L., F.Y., X.M., X.J., and Y.Z.; Data curation, W. L., F.Y., X.J., and Y.Z.; Writing-original draft preparation, W.L., and Y.Z.; Writing-review and editing, W.L., F.Y., X.J and Y.Z.; Supervision, X.J., and Y.Z.; Project administration, Y.Z.; Funding acquisition, X.J. and Y.Z.;

Funding: This work was supported by grants from the Xijing Hospital (XJZT21CM07) and the National Natural Science Foundation of China (No. 82171458).

Conflicts of Interest: The authors declare no conflict of interest.

References

1. Huse, J. T. & Holland, E. C. Targeting brain cancer: advances in the molecular pathology of malignant glioma and medulloblastoma. Nat Rev Cancer 10, 319–331, doi:10.1038/nrc2818 (2010).
2. Stupp, R. et al. Radiotherapy plus concomitant and adjuvant temozolomide for glioblastoma. N Engl J Med 352, 987–996, doi:10.1056/NEJMoa043330 (2005).
3. Ahir, B. K., Engelhard, H. H. & Lakka, S. S. Tumor Development and Angiogenesis in Adult Brain Tumor: Glioblastoma. Mol Neurobiol 57, 2461–2478, doi:10.1007/s12035-020-01892-8 (2020).

4. Winkler, F. Hostile takeover: how tumours hijack pre-existing vascular environments to thrive. J. Pathol. 242, 267–272 doi:10.1002/path.4904 (2017)
5. van Tellingen, O. *et al.* Overcoming the blood-brain tumor barrier for effective glioblastoma treatment. Drug Resist Updat 19, 1–12, doi:10.1016/j.drup.2015.02.002 (2015).
6. Zhao, Z., Nelson, A. R., Betsholtz, C. & Zlokovic, B. V. Establishment and Dysfunction of the Blood-Brain Barrier. Cell 163, 1064–1078, doi:10.1016/j.cell.2015.10.067 (2015).
7. Harris A. L. (1997). Antiangiogenesis for cancer therapy. *Lancet*, 349 Suppl 2, SII13–SII15. doi:10.1016/s0140-6736(97)90014-3 (1997)
8. Verhoeff, J. J. *et al.* Concerns about anti-angiogenic treatment in patients with glioblastoma multiforme.*BMC cancer* 9, 444. https://doi.org/10.1186/1471-2407-9-444.(2009)
9. Gilbert, M. R. Antiangiogenic therapy for glioblastoma: complex biology and complicated results. J. Clin. Oncol. 34, 1567–1569, doi:10.1200/JCO.2016.66.5364 (2016).
10. Tang, N. & Ostap, E. M. Motor domain-dependent localization of myo1b (myr-1). Current biology: CB 11, 1131–1135, doi:10.1016/s0960-9822(01)00320-7 (2001).
11. Hartman, M. A. & Spudich, J. A. The myosin superfamily at a glance. Journal of cell science 125, 1627–1632, doi:10.1242/jcs.094300 (2012).
12. Mentes, A. *et al.* High-resolution cryo-EM structures of actin-bound myosin states reveal the mechanism of myosin force sensing. Proceedings of the National Academy of Sciences of the United States of America 115, 1292–1297, doi:10.1073/pnas.1718316115 (2018).
13. Yamada, A. *et al.* Catch-bond behaviour facilitates membrane tubulation by non-processive myosin 1b. Nature communications 5, 3624, doi:10.1038/ncomms4624 (2014).
14. Chapman, B. V. *et al.* MicroRNA-363 targets myosin 1B to reduce cellular migration in head and neck cancer. BMC cancer 15, 861, doi:10.1186/s12885-015-1888-3 (2015).
15. Xie, S. *et al.* Construction of a hypoxia-immune-related prognostic model and targeted therapeutic strategies for cervical cancer. Int Immunol 34, 379–394, doi:10.1093/intimm/dxac017 (2022).
16. Goveia, J. *et al.* An Integrated Gene Expression Landscape Profiling Approach to Identify Lung Tumor Endothelial Cell Heterogeneity and Angiogenic Candidates. Cancer Cell. 37(1):21–36.e13. doi:10.1016/j.ccell.2019.12.001 (2020)..
17. Xie, Y. et al. Key molecular alterations in endothelial cells in human glioblastoma uncovered through single-cell RNA sequencing. JCI insight, 6(15), e150861.doi:10.1172/jci.insight.150861.(2021).
18. Li, X., Hu, J., Zhao, X., Li, J. & Chen, Y. Piezo channels in the urinary system. Exp Mol Med 54, 697–710, doi:10.1038/s12276-022-00777-1 (2022).
19. Lai, A. *et al.* Mechanosensing by Piezo1 and its implications for physiology and various pathologies.Biol Rev Camb Philos Soc. 97(2):604–614. (2022).
20. Giu, T. T. *et al.* Piezo1-Mediated Ca(2+) Activities Regulate Brain Vascular Pathfinding during Development. *Neuron* 108, 180–192 e185, doi:10.1016/j.neuron.2020.07.025 (2020).

21. Li, J. *et al.* Piezo1 integration of vascular architecture with physiological force. Nature 515, 279–282, doi:10.1038/nature13701 (2014)
22. McHugh, B. J., Murdoch, A., Haslett, C. & Sethi, T. Loss of the integrin-activating transmembrane protein Fam38A (Piezo1) promotes a switch to a reduced integrin-dependent mode of cell migration. PLoS One 7, e40346, doi:10.1371/journal.pone.0040346 (2012).
23. Richards, T. A. & Cavalier-Smith, T. Myosin domain evolution and the primary divergence of eukaryotes. Nature 436, 1113–1118, doi:10.1038/nature03949 (2005)
24. Hudspeth AJ. How the ear's works work: mechanoelectrical transduction and amplification by hair cells. C R Biol 328(2):155–62 (2005)
25. Jiang, Y. *et al.* Targeting extracellular matrix stiffness and mechanotransducers to improve cancer therapy. J Hematol Oncol 15, 34, doi:10.1186/s13045-022-01252-0 (2022)
26. Orsini, E. M. *et al.* Stretching the Function of Innate Immune Cells. Front Immunol 12, 767319, doi:10.3389/fimmu.2021.767319 (2021)
27. Jiang, Y. *et al.* Glioblastoma Cell Malignancy and Drug Sensitivity Are Affected by the Cell of Origin. Cell reports 18(4), 977–990 (2017).
28. Ballabh, P. *et al.* The blood-brain barrier: an overview: structure, regulation, and clinical implications Factors influencing the blood-brain barrier permeability. Neurobiology of disease 16(1), 1–13. doi:10.1016/j.nbd.2003.12.016 (2004)
29. Zimna, A. & Kurpisz, M. Hypoxia-Inducible Factor-1 in Physiological and Pathophysiological Angiogenesis: Applications and Therapies. *Biomed Res Int* 2015, 549412, doi:10.1155/2015/549412 (2015)
30. Olsson, A. K., Dimberg, A., Kreuger, J. & Claesson-Welsh, L. VEGF receptor signalling - in control of vascular function. Nature reviews. Molecular cell biology 7, 359–371, doi:10.1038/nrm1911 (2006)
31. De Bock, M. *et al.* Endothelial calcium dynamics, connexin channels and blood-brain barrier function. Prog Neurobiol 108, 1–20, doi:10.1016/j.pneurobio.2013.06.001 (2013)
32. Yang, Q. *et al.* Candidate Biomarkers and Molecular Mechanism Investigation for Glioblastoma Multiforme Utilizing WGCNA. *Biomed Res Int* 2018, 4246703, doi:10.1155/2018/4246703 (2018)
33. Zhang, X. *et al.* Piezo1-mediated mechanosensation in bone marrow macrophages promotes vascular niche regeneration after irradiation injury. Theranostics 12, 1621–1638, doi:10.7150/thno.64963 (2022).
34. Hanahan, D., & Weinberg, R. A. Hallmarks of cancer: the next generation. Cell 144(5), 646–674 (2011).
35. Ahir, B. K., Engelhard, H. H. & Lakka, S. S. Tumor Development and Angiogenesis in Adult Brain Tumor: Glioblastoma. Mol Neurobiol 57, 2461–2478, doi:10.1007/s12035-020-01892-8 (2020)
36. Viallard, C. & Larrivee, B. Tumor angiogenesis and vascular normalization: alternative therapeutic targets. Angiogenesis 20, 409–426, doi:10.1007/s10456-017-9562-9 (2017).

37. Seano, G. & Jain, R. K. Vessel co-option in glioblastoma: emerging insights and opportunities. Angiogenesis 23, 9–16, doi:10.1007/s10456-019-09691-z (2020)
38. Wick, W. *et al.* Lomustine and Bevacizumab in Progressive Glioblastoma. N Engl J Med 377, 1954–1963, doi:10.1056/NEJMoa1707358 (2017)
39. Komaba, S. & Coluccio, L. M. Myosin 1b Regulates Amino Acid Transport by Associating Transporters with the Apical Plasma Membrane of Kidney Cells. PloS one 10, e0138012, doi:10.1371/journal.pone.0138012 (2015)
40. Veigel, C. *et al.* The motor protein myosin-I produces its working stroke in two steps. Nature 398, 530–533, doi:10.1038/19104 (1999).
41. Prosperi, M. T. *et al.* Myosin 1b functions as an effector of EphB signaling to control cell repulsion. The Journal of cell biology 210, 347–361, doi:10.1083/jcb.201501018 (2015).
42. Adamek, N., Lieto-Trivedi, A., Geeves, M. A. & Coluccio, L. M. Modification of loop 1 affects the nucleotide binding properties of Myo1c, the adaptation motor in the inner ear. Biochemistry 49, 958–971, doi:10.1021/bi901803j (2010).
43. Batters, C., Wallace, M. I., Coluccio, L. M. & Molloy, J. E. A model of stereocilia adaptation based on single molecule mechanical studies of myosin I. Philosophical transactions of the Royal Society of London. Series B, Biological sciences 359, 1895–1905, doi:10.1098/rstb.2004.1559 (2004).
44. Delestre-Delacour, C. *et al.* Myosin 1b and F-actin are involved in the control of secretory granule biogenesis. Scientific reports 7, 5172, doi:10.1038/s41598-017-05617-1 (2017)
45. Makowska, K. A., Hughes, R. E., White, K. J., Wells, C. M. & Peckham, M. Specific Myosins Control Actin Organization, Cell Morphology, and Migration in Prostate Cancer Cells. Cell reports 13, 2118–2125, doi:10.1016/j.celrep.2015.11.012 (2015).
46. Shimonosono, M. *et al.* Molecular pathogenesis of esophageal squamous cell carcinoma: Identification of the antitumor effects of miR1453p on gene regulation. International journal of oncology 54, 673–688, doi:10.3892/ijo.2018.4657 (2019).
47. Shellenberger, N. W., Collinsworth, K. K., Subbiah, S., Klein, D. & Neary, J. M. Hypoxia induces an increase in intestinal permeability and pulmonary arterial pressures in neonatal Holstein calves despite feeding the flavonoid rutin. J Dairy Sci 103, 2821–2828, doi:10.3168/jds.2019-17289 (2020)
48. Goel, H. L. & Mercurio, A. M. VEGF targets the tumour cell. Nature reviews. Cancer 13, 871–882, doi:10.1038/nrc3627 (2013).
49. Fong, G. H., Rossant, J., Gertsenstein, M. & Breitman, M. L. Role of the Flt-1 receptor tyrosine kinase in regulating the assembly of vascular endothelium. Nature 376, 66–70, doi:10.1038/376066a0 (1995).
50. Dhanasekaran, R. *et al.* The MYC oncogene - the grand orchestrator of cancer growth and immune evasion. Nat Rev Clin Oncol 19, 23–36, doi:10.1038/s41571-021-00549-2 (2022).
51. Bretones, G., Delgado, M. D. & Leon, J. Myc and cell cycle control. Biochim Biophys Acta 1849, 506–516, doi:10.1016/j.bbagrm.2014.03.013 (2015)

52. Zhang, X. *et al.* N-myc Downstream-Regulated Gene 1 (NDRG1) Regulates Vascular Endothelial Growth Factor A (VEGFA) and Malignancies in Glioblastoma Multiforme (GBM). *Biomed Res Int* 2022, 3233004, doi:10.1155/2022/3233004 (2022).
53. Coste, B. *et al.* Piezo1 and Piezo2 are essential components of distinct mechanically activated cation channels. Science 330, 55–60, doi:10.1126/science.1193270 (2010)

Figures

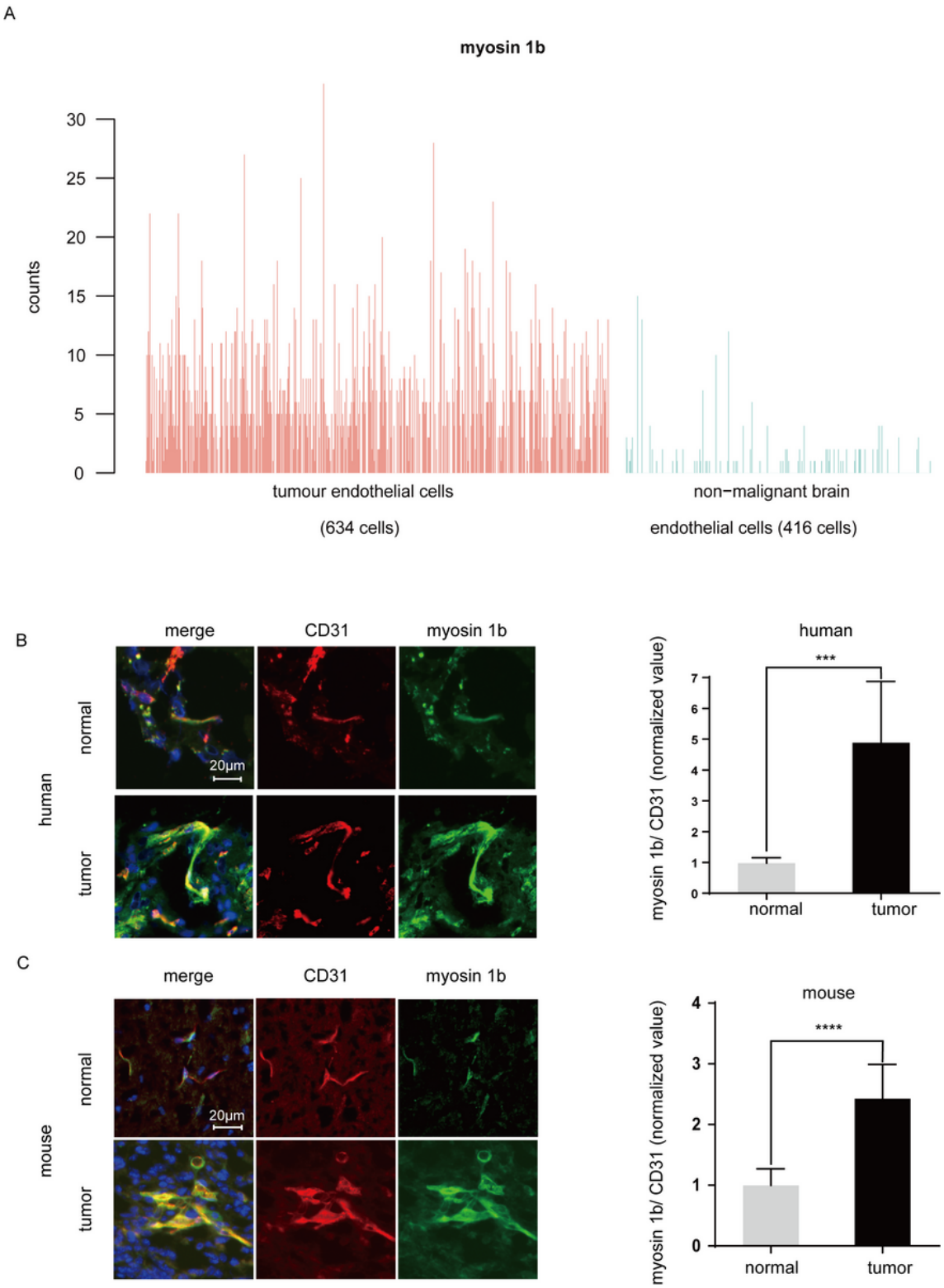

Figure 1

Myosin 1b is upregulated in GBM ECs. (A) Bar plots showing myosin 1b expression in endothelial cells in GBM (red) and non-malignant brain endothelial cells (blue) (GSE162631) (Student's t-test; $p < 0.0001$). (B-C) The expression of myosin 1b and CD31 in normal and tumor tissues were detected in patient (tumor n=10; normal n=6) and in mice (tumor n=10; normal n=10) GBM samples by immunohistochemical staining. The data are presented as the mean ± SD. $P < 0.001$, ***; $P < 0.0001$, ****.

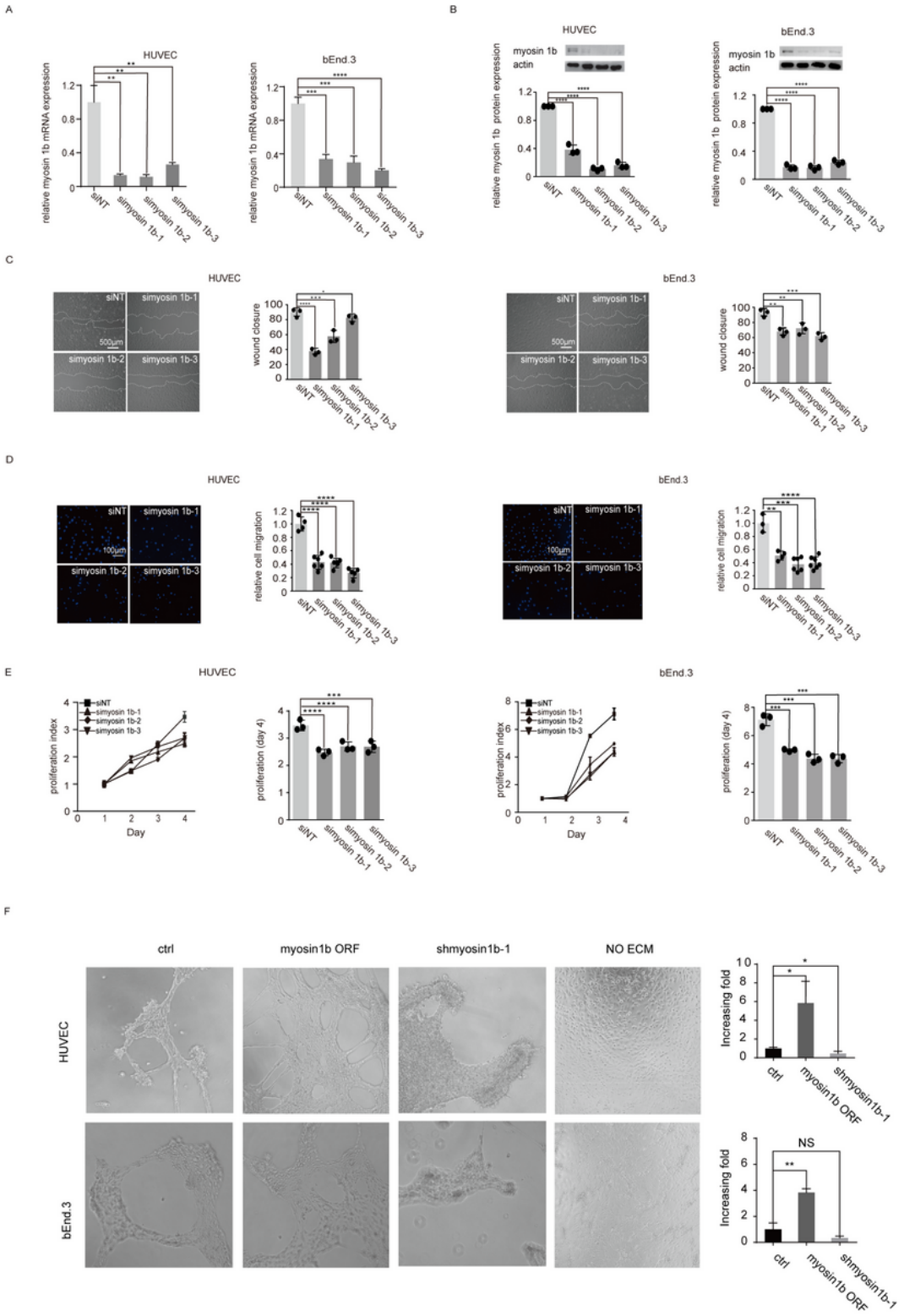

Figure 2

Myosin 1b promotes brain EC proliferation, migration and tube formation. (A and B) HUVEC and bEnd.3 cells transfected with myosin 1b knock-down or empty control plasmids were investigated by real-time PCR and western blot assay (for HUVEC, n=3 respectively; for bEnd.3, n=3 respectively). (C, D and E) Regulation of myosin 1b on proliferation and migration were confirmed by wound healing analysis (for HUVEC, n=3 respectively; for bEnd.3, n=3 respectively), transwell assay (for HUVEC, n=4, 6, 6, 5

respectively; for bEnd.3, n=3, 4, 6, 7 respectively) and cck-8 analysis (for HUVEC, n=3 respectively; for bEnd.3, n=3 respectively). (F) Tube formation of HUVEC or bEnd.3 cells were tested after myosin 1b overexpressing or silencing. Nucleus is in blue. The data are presented as the mean ± SD. P < 0.05, *; P < 0.01, **; P < 0.001, ***; P < 0.0001, ****.

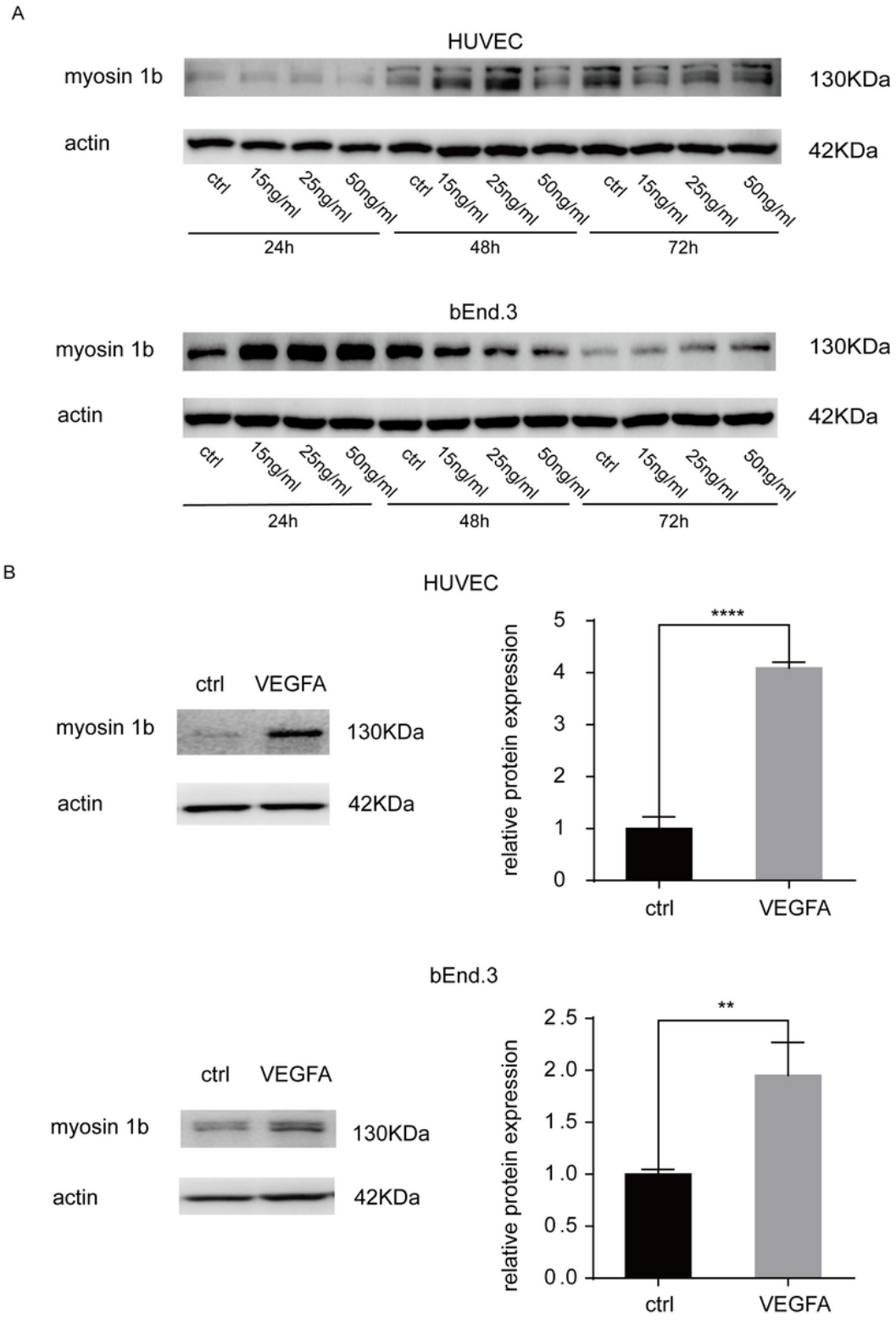

Figure 3

VEGF promotes myosin 1b expression in human and mouse brain ECs (A) The expression level of myosin 1b was evaluated by western blot in HUVEC or bEnd.3 cells after treatment with VEGFA at different concentrations and time points . (B) HUVEC cells were treated with VEGFA at the concentration of 25 ng/ml for 48 hours; bEnd.3 cells were treated with VEGFA at the concentration of 25 ng/ml for 24 hours.The expression level of myosin 1b was then detected by western blot (n=3 respectively for all quantifications)

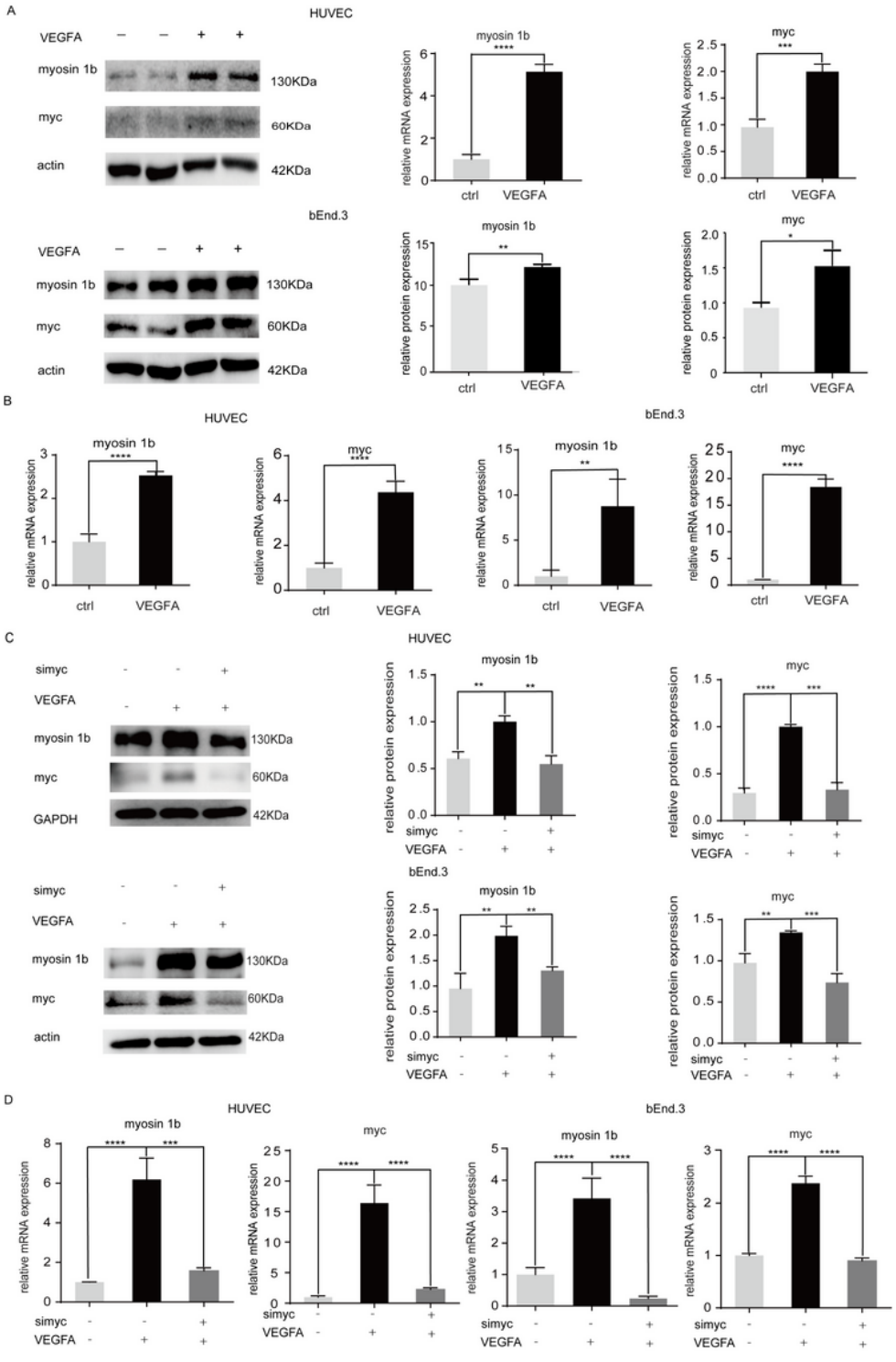

Figure 4

VEGF promotes myosin 1b expression via myc. (A) HUVEC cells were treated with VEGFA at the concentration of 25 ng/ml for 48 hours; bEnd.3 cells were treated with VEGFA at the concentration of 25 ng/ml for 24 hours.The expression level of myosin 1b and myc was then detected by western blot (n=3 respectively). (B) The transcriptional level of myosin 1b and myc was evaluated in HUVEC (n=6 respectively) and in bEnd3 cells (n=4 respectively) after VEGFA treatment by real-time PCR. (C) HUVEC cells were transiently transfected with shmyc-2 and then treated with VEGFA at 25 ng/ml for 48 hours; bEnd.3 cells were transiently transfected with shmyc-1 and then treated with VEGFA at 25 ng/ml for 24 hours. The expression level of myosin 1b and myc were analyzed by western blot assay (n=3 respectively). (D) The transcriptional level of myosin 1b and myc was detected by real-time PCR in HUVEC (C) (n=4 respectively) and bEnd.3 cells (n=6, 6, 5 respectively). The data are presented as the mean ± SD. $P < 0.05$, *; $P < 0.01$, **; $P < 0.001$, ***; $P < 0.0001$, ****.

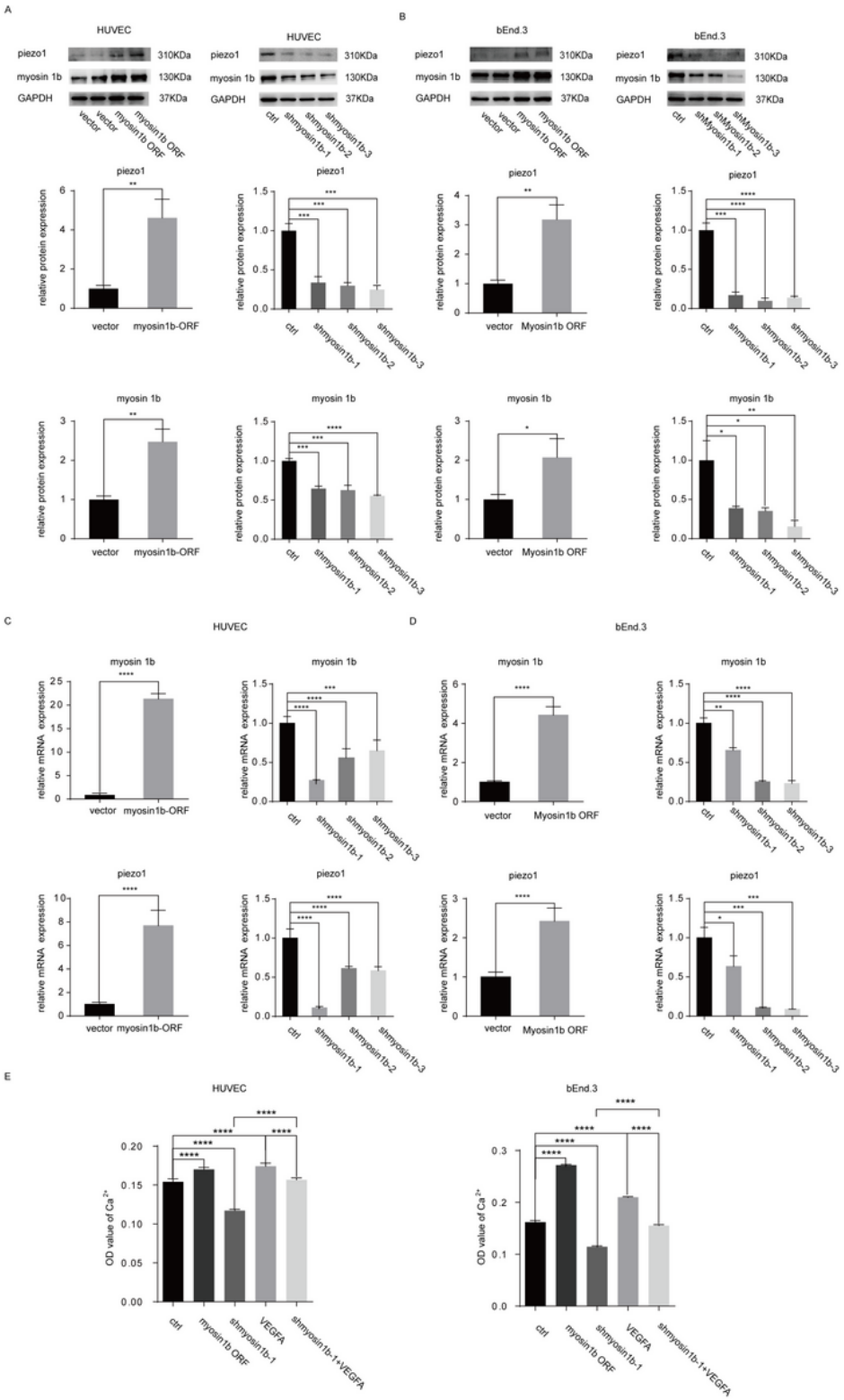

Figure 5

Myosin 1b promotes Piezo1 expression and calcium influx in ECs. (A) The expression level of Piezo1 was detected by western blot in HUVEC cells with constitutive myosin1b overexpression or knockdown (n=3 respectively for the columns of the quantification). The myosin 1b expression is verified in the HUVEC cells. (B) The expression level of Piezo1 in bEnd.3 cells with constitutive myosin1b overexpression or knockdown was detected by western blot (n=3 respectively for the columns of the quantification). The

myosin 1b expression is verified in the bEnd.3 cells. The transcriptional level of myosin 1b and Piezo1 was detected by real-time PCR in HUVEC (C) (n=6 respectively) and bEnd.3 cells (D) (n=6 respectively). The level of intracellular Ca^{2+} content was detected in the specified conditions in HUVEC (F) or bEnd.3 cells (F). Data are presented as the mean ± SD. P < 0.05, *; P < 0.01, **; P < 0.001, ***; P < 0.0001, ****.

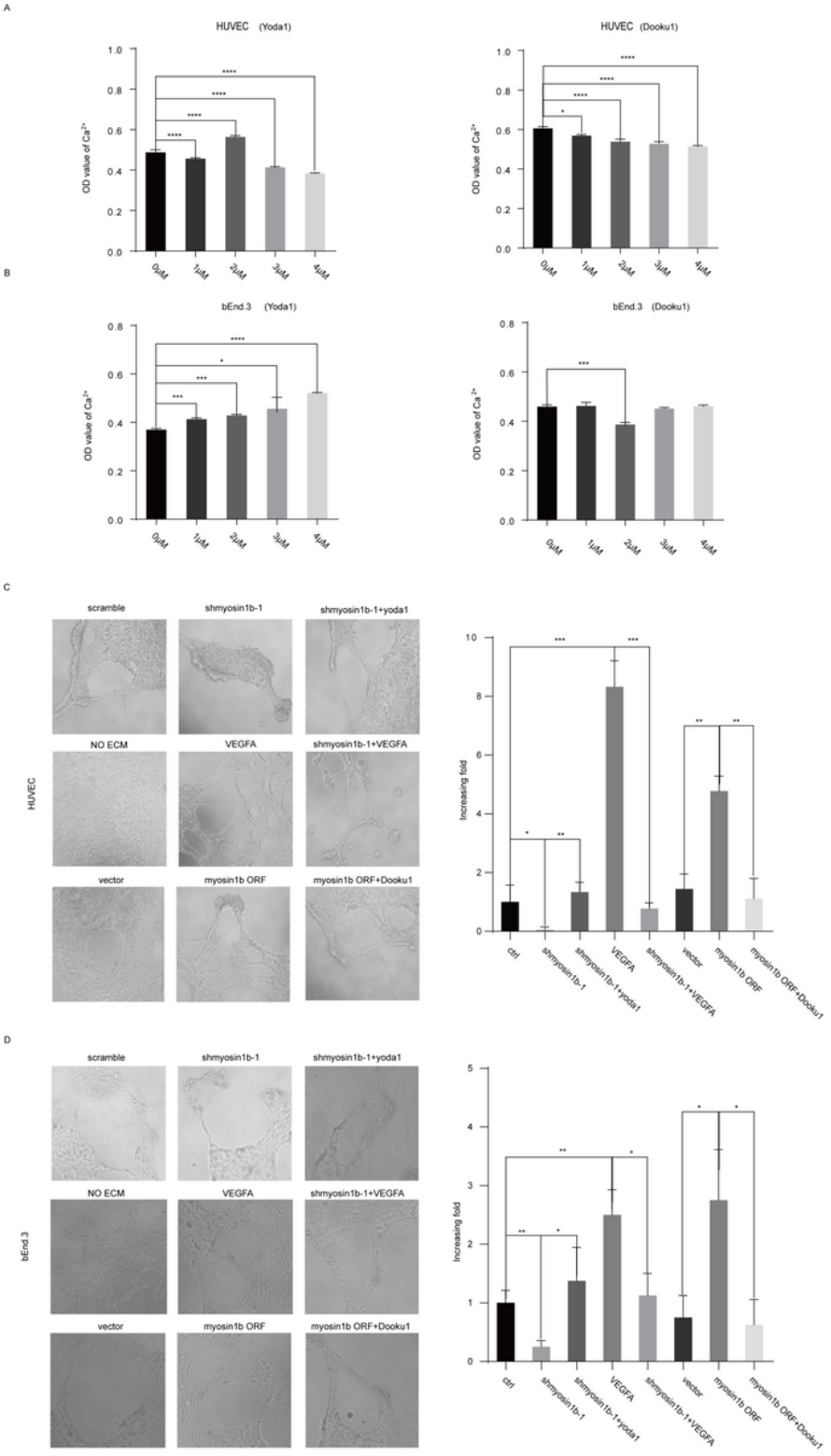

Figure 6

Myosin1b promotes angiogenesis via Piezo1 and VEGFA can be the trigger. (A) HUVEC cells were treated with Yoda1 and Dooku1 for 24 hours at different concentration. The level of intracellular calcium content was determined according to the optical density (OD) value(n=6 respectively). (B) bEnd.3 cells were treated with Yoda1 and Dooku1 for 24 hours at different concentration. The intracellular calcium content was detected. (n=6 respectively). (C) and (D) ECs with or without constitutive myosin1b knockdown or overexpression were treated with VEGFA at 25 ng/ml, Yoda1 at 2μM for HUVEC and at 4μM for bEnd.3, or Dooku1 at 4μM for HUVEC and at 2μM for bEnd.3. Cells were incubated in a humidified incubator at 37 °C with 5% CO_2 and 95% air for 24 hours for the tube formation assay. Data are presented as the mean ± SD. P < 0.05, *; P < 0.01, **; P < 0.001, ***; P < 0.0001, ****.

Supplementary Files

This is a list of supplementary files associated with this preprint. Click to download.

- mechanism.png
- supplement.docx
- supplementalfigure1.tif
- supplementalfigure2.tif